Chinese Journal of
POLYMER SCIENCE

FEATURE ARTICLE

https://doi.org/10.1007/s10118-018-2035-9
Chinese J. Polym. Sci. 2018, 36, 273–287

Functionally Oriented Tumor Microenvironment Responsive Polymeric Nanoassembly: Engineering and Applications

Wen-Ming Zhang[†], Jian Zhang[†], Zhu Qiao, and Jun Yin[*]

Department of Polymer Science and Engineering, School of Chemistry and Chemical Engineering, Hefei University of Technology and Anhui Province Key Laboratory of Advanced Catalytic Materials and Reaction Engineering, Hefei 230009, China

Abstract The excellent drug encapsulation, prolonged *in vivo* circulation time, enhanced pharmacokinetics, and reduced adverse effects make the polymeric assemblies ideal carriers in nanomedicine, and become an emerging research field with rapid development. *In vivo*, the polymer nanoassemblies will experience five steps, including circulation in the blood, accumulation in the tumoral site, penetration into the deep tumor tissue to reach cancer cells, internalization into cancer cells, and intracellular drug release. However, although tremendous efforts have been made to the material design, currently available carriers still have difficulties in fulfilling all of the requirements. Moreover, the long-standing dilemma of the synchronized stability and permeability of vesicles is still a big challenge, which confused researchers for a long time. This feature article focuses on the recent progress of single- or multi-stimuli triggered theranostic platforms, and the extracellularly reengineered shell-sheddable polymeric nanocarriers are systematically discussed. The perspectives for future developments in the nanocarriers functioned with artificial helical polymers (the potential cell-penetrating peptides mimics) are also proposed. We speculate that this feature article can fit the interesting of diverse readers and a guideline for the design of next generation of drug nanocarriers.

Keywords Block copolymers; Tumor microenvironment responsive; Self-assembly; Theranostic; Nanomedicine

Citation: Zhang, W. M.; Zhang, J.; Qiao, Z.; Yin, J. Functionally Oriented Tumor Microenvironment Responsive Polymeric Nanoassembly: Engineering and Applications. Chinese J. Polym. Sci. 2018, 36(3), 273–287.

INTRODUCTION

With the gradual deterioration of our living environment and the accumulation of personal bad habits, the cancerous types and patients exhibit a rising trend, which seriously affect people's normal lives. Up to now, tremendous tactics, including surgery, chemotherapy, and radiotherapy, have been already developed to deal with such one of the greatest enemies of mankind, but inevitable adverse effects and low therapeutic efficacies always exist during cancer treatment. For example, the low solubility, undesirable biodistribution, poor pharmacokinetics, inability to target the affected sites, inefficient cellular uptake, and indiscriminate killing of both cancerous and healthy tissues/cells are several major obstacles in the chemotherapy with the aid of small molecular anticancer drugs[1, 2]. Such undesired side effects and inherent systemic and cellular barriers would greatly reduce the therapeutic outcome, and the possible multidrug resistance to a special type of tumor might further decrease the therapeutic efficacy.

To address these limitations, polymeric assemblies (PAs) with stimuli (pH, redox, enzyme, temperature, light, hypoxia, and electromagnetic field) regulated physicochemical properties and tailor-made functions fabricated from stimuli-responsive copolymers, like amphiphilic block copolymers and double hydrophilic block copolymers, can response and adapt to various factors and situations, which have long been the researchers' focus[3–16]. Moreover, PAs can offer a highly integrated platform in biomedical exploration due to their good drug encapsulation, prolonged *in vivo* circulation time, enhanced bioavailability and pharmacokinetics of therapeutics, reduced adverse effects, and minimal damage to normal tissues if targeting function was introduced[17, 18]. All of these remarkable advantages endow them with enormous promising for cancer diagnosis and therapy. To date, a certain number of polymeric nanomedicines have entered clinical application or in stages of clinical trials[19–22].

Traditional polymeric nanomedicines are typically prepared *via* either physical encapsulation or covalent conjugation. Covalent conjugation is always realized through the polymerization of post-modified monomers with contrast agent or drug pendants, leading to better stability so that contrast agents or drugs do not tend to undergo burst release. On the other hand, physical encapsulation can be generated using nanoprecipitation, co-solvent self-assembly, or electrostatic interaction *etc*. However, the physical encapsulation of drugs sometimes suffers from undesired leaking if in a diluted condition, which remains a problem in cancer therapy. No matter whether physical encapsulation or

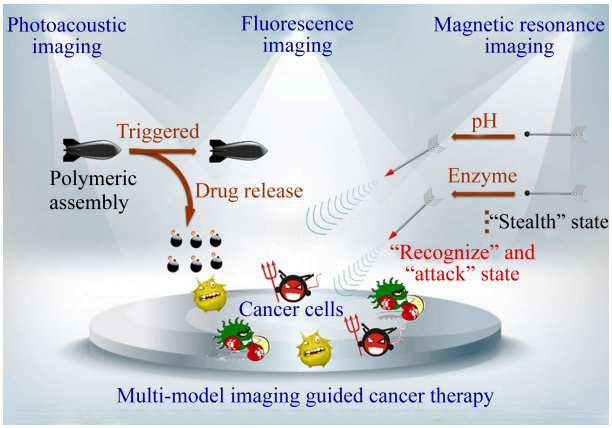
[*] Corresponding author: E-mail yinjun@hfut.edu.cn
[†] These authors contributed equally to this work.
Invited paper for special issue of "Supramolecular Self-Assembly"
Received August 17, 2017; Accepted September 5, 2017; Published online December 20, 2017

© Chinese Chemical Society
Institute of Chemistry, Chinese Academy of Sciences
Springer-Verlag GmbH Germany, part of Springer Nature 2018

covalent conjugation, one can still encapsulate single or multiple contrast agents and drugs within PAs for the follow-up diagnostic and treatment.

As we know, after an intravenous injection of polymeric nanomedicines, the PAs will experience five steps[23, 24], including circulation in the blood (step 1), accumulation in the tumor (step 2), penetration into the deep tumor tissue to reach cancer cells (step 3), internalization into cancer cells (step 4), and intracellular drug release (step 5). To keep the individual stability of PAs and extend the blood circulation time, the susceptible interactions between PAs and blood plasma proteins must be avoided. Thus, biocompatible hydrophilic polymer should be anchored on the surface of corresponding PAs. Among them, poly(ethylene glycol) (PEG), poly(2-meth-acryloyloxyethyl phosphorylcholine) (PMPC), poly(2-hydroxypropyl methacrylate) (PHPMA), and poly(carboxybetaine) are always used because of their protein-resistant and the bypassing of recognition and capture by the reticuloendothelial system (RES) or mononuclear phagocyte system (MPS)[25, 26]. Moreover, to ensure the therapeutic efficiency, it is important to avoid any low efficiency steps and maximize the efficiency of each step to achieve high overall efficiency. PAs with large sizes are reported to favor long time blood circulation, but, in contrast, small PAs are more easy to accumulate in tumor tissues by enhanced permeability and retention (EPR) effect due to the pathologically leaky vasculature and enhance the subsequent penetration into deep tumor tissue to reach the cancer cells.

The different needs in the first three steps (steps 1–3) of high efficiency cancer therapy are presented and even discussed about the opposite cases. Thus, the way how to engineer PAs to fit each step and effectively exert their therapeutic efficacy is the key point to design the next generation polymeric nanomedicines. Herein, this feature article highlights the new progress in multi-model imaging guided cancer therapy (Scheme 1), especially several representatives of extra- and intra-cellularly reengineered stimuli-responsive PAs in tumor tissue for intelligent cell imaging and drug delivery. The perspectives for future developments are also discussed. We hope that this article will attract the interest of diverse readers in the field of chemical, biological, and medical science, and provide a guideline for the design of next generation of drug nanocarriers.



Scheme 1 Schematic illustration of multi-model imaging guided cancer therapy, and extra- and intra-cellularly reengineered stimuli-responsive transformable polymeric assemblies in tumor tissue for intelligent cancer treatment

FOR STEPS 1–3

To overcome the contradiction between blood circulation and tumor accumulation and penetration, regulation of the nanomedicine surface property is a newly emerging protocol. During blood circulation, PAs should be stable for a long time to give enough opportunity for tumor accumulation and minimize their interaction with MPS to avoid the rapid clearance by RES. Then, they should be changed to easily adapted state, such as smaller size, while remaining in tumor tissues for deeper tumor penetration. As soon as the PAs reach cancer cells after deep tumor penetration, they must be able to interact with and stick to cancer cells for efficient cellular uptake. To realize this assumption, several research groups have carried out excellent works. Typically, the "shielding processes" with the aid of PEGylation or small molecule cages were performed to modify the surface of PAs[27–33]. The resultant shell-sheddable PAs had been proved to be stealthy during blood circulation but change their properties (surface charge, particle size, or caged-uncaged ligand transition) to accumulate at tumor tissues through passive or active targeting. Moreover, compared with the EPR effect in passive targeting strategy, active targeting is a much better direction of modern nanocarrier design. By taking advantage of this concept, TAT (transactivator of transcription) peptide[34], a type of cell-penetrating peptide (CPP) that can greatly enhance the cell uptake of nanocarriers, and folic acid (FA)[35], a type of targeting primitives with high affinity to the folate receptor, were designed to be in inactive state in the initial stage. Then, once accumulated in the tumor tissues, the masked targeting primitives were reactivated by the tumor microenvironment. Such extracellularly reengineered processes are always triggered by the extracellular stimuli to specific linkages or interactions introduced into the PAs previously.

It has been confirmed that cationic charges are shown to improve tumor penetration, while a neutral or a slightly negatively charged surface favors a long blood circulation[36–41]. But the nonspecificities of cations always result in serious adsorption by proteins or clearance by monocytes in blood. Thus, this kind of demand gives birth to the electrostatic interaction mediated reversibly PEGylated PAs for tumor penetration and cellular internalization. As a typical example reported by Sethuraman and Bae, a drug targeting composite for acidic tumors based on ultra pH-sensitive polymer and cell penetrating TAT was developed[42]. Firstly, a TAT micelle with a hydrophobic core made of poly(L-lactic acid) (PLLA) and a hydrophilic shell consisting of polyethylene glycol (PEG) conjugated to TAT was formed. Then, the complexation between the positively charged TAT micelle and negatively charged ultra pH-sensitive diblock copolymer of poly(methacryloyl sulfadimethoxine)-block-PEG (PSD-*b*-PEG) was carried on to give the final drug-loaded PAs. The results of flow cytometry and confocal microscopy showed that the higher

https://doi.org/10.1007/s10118-018-2035-9

uptake of TAT micelles occurred at pH = 6.6 compared to pH = 7.4 indicating the shielding of TAT at normal pH and deshielding at tumor pH (Fig. 1). Moreover, TAT was not only translocated into the cells but was also seen on the surface of the nucleus. These results strongly indicated that the TAT micelles could be able to deliver any hydrophobic drug near the nucleus.

As literatures illustrated, PAs with diameters less than 200 nm favor tumor accumulation *via* EPR effect due to their superior tumor tissue penetration[43–46]. But, in the tumor tissues composed of tightly packed cells, they are too large to diffuse into the internal. Thus, the small nanocarriers are needed in this situation to penetrate the dense tumors. Sun *et al.* recently constructed a "cluster-bomb" type of dendrimer@lipid nanoassembly to achieve this goal[47]. A pH-sensitive sixth-generation nontoxic polyaminoester dendrimer (~5 nm) with a drug loading capacity was chosen as the "bomblet"; the lipid shell could keep the nanoassembly stable and stealthy in the blood. The whole dendrimer@lipid nanoassembly was ~45 nm in diameter and contained ~25 dendrimers. Once the "cluster-bomb" nanoassembly accumulated in the tumor site *via* the EPR effect, fusion of the lipid layer with the cell membrane would release the dendrimers. The small dendrimers in extracellular fluid further penetrated into the tumor internal, letting the dendrimer surface be protonated (pH: 6–7) and become positively charged, which could efficiently trigger fast cellular uptake. Once in the lysosomes, the dendrimers became soluble in the lower pH microenvironment and released encapsulated drugs (Fig. 2).

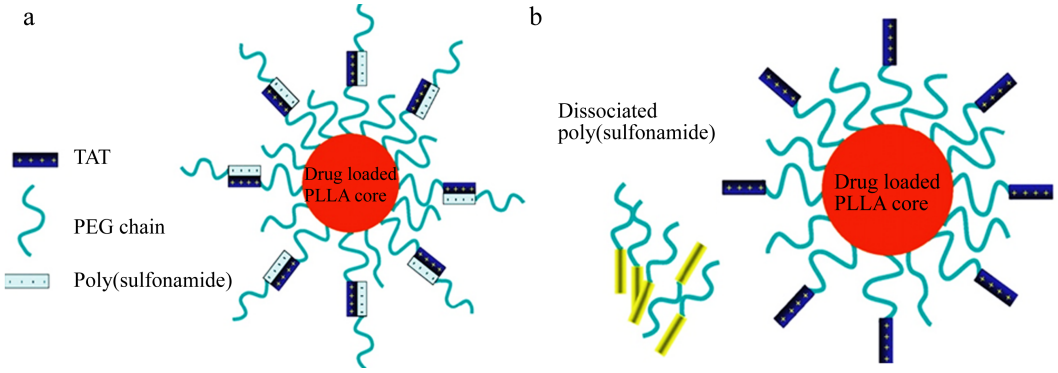


Fig. 1 Schematic model for the proposed drug delivery system: the carrier system consisting of two components, a PLLA-*b*-PEG micelle conjugated to TAT and a pH-sensitive diblock polymer PSD-*b*-PEG: (a) At normal blood pH, the sulfonamide is negatively charged, and when mixed with the TAT micelle, shields the TAT by electrostatic interaction. Only PEG is exposed to the outside which could make the carrier long circulating; (b) When the system experiences a decrease in pH (near tumor) sulfonamide loses charge and detaches, thus exposing TAT for interaction with tumor cells. (Reproduced with permission from Ref. [42]; Copyright (2007) Elsevier)

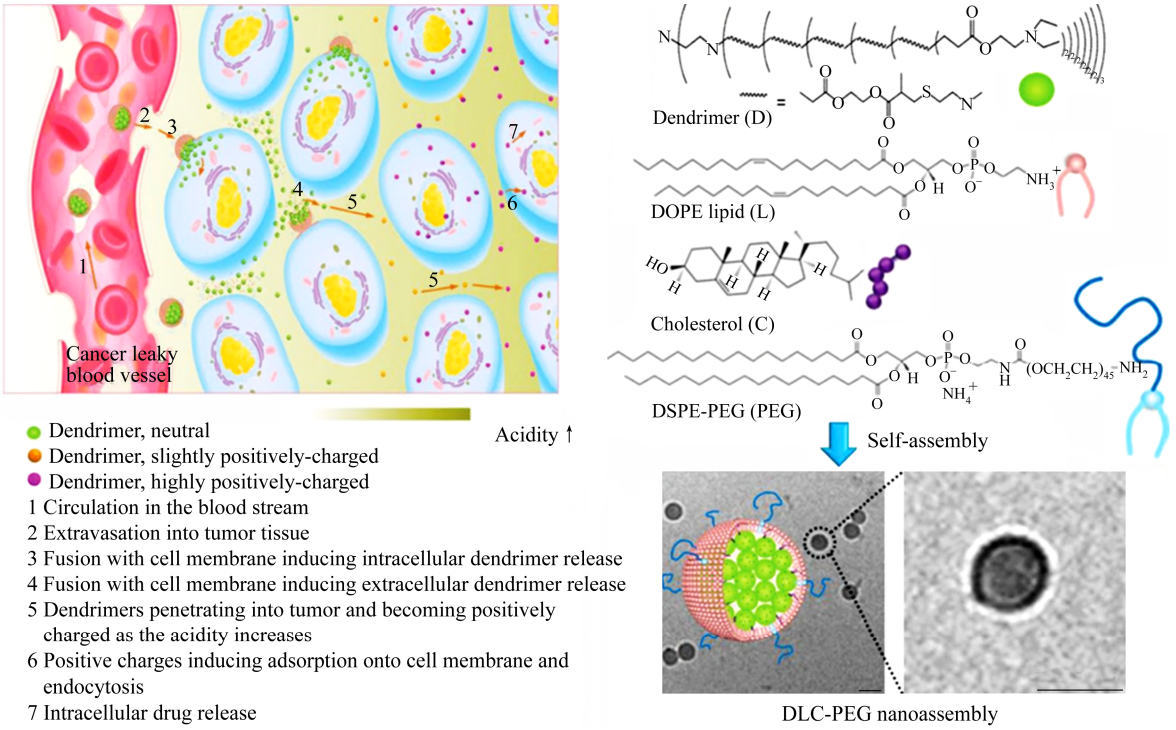


Fig. 2 Schematic of the "cluster-bomb" like nanoassembly and how it works (The nanoassembly structure with a dendrimer core and lipidic shell was confirmed by cryo-TEM imaging.) (Reproduced with permission from Ref. [47]; Copyright (2014) John Wiley and Sons)

https://doi.org/10.1007/s10118-018-2035-9

Aside from the tumor acidity triggered extracellular reengineering, the certain enzymes, for example, matrix metalloproteinases (MMPs; particularly, MMP-2) overexpress in the extracellular matrix is another powerful tool to cleave the linkers on the core-shell interface of shell-sheddable PAs to change the corresponding surface properties and enhance subsequent enzyme-responsive delivery of therapeutic agents[48–52]. Enzyme-catalyzed reactions are always highly selective and efficient toward specific substrates under mild conditions. As a typical example, Gullotti *et al.* immobilized a cell-interactive TAT peptide (RKKRRQRRR) and a PEGpeptide-conjugate on PLGA core to obtain cell interactive nanoparticles with a removable PEG layer, called peritumorally activatable nanoparticle (PANP) (Fig. 3a)[53]. The PEG was conjugated to a MMP-substrate peptide (GPLGVRGC), serving as the MMP-2 cleavable linker. As the cleavage of PEG in the tumoral environment, the TAT peptide was exposed and enabled the nanoparticles to actively engage with tumor cells. To test the effect of TAT peptide and MMP-2 sensitivity, cellular uptake and biological activity of the nanoparticles were also tested *in vitro*. The dual-modified PANPs exhibited MMP-2 dependent cellular uptake compared with the untreated ones (Fig. 3b).

Alternatively, small molecule cages have also been applied in the reengineering of protected ligands through stimuli-responsive cleavable covalent linkages. When the PAs accumulate at the tumor site, the small targeting ligands are removed[54–57]. Then, the ligand modified surfaces are reactivated and exposed to the outside, which can further improve the cell uptake of the PAs. For example, Li *et al.* explored a nanoparticle (^{DA}TAT-NP$_{IR\&DOX}$) with tumor acidity activated TAT as well as a NIR dye IR-780 and doxorubicin (DOX) contained flexible chain polyphosphoester core[54]. The resultant transformable ^{DA}TAT-NP$_{IR\&DOX}$ nanoparticles could efficiently avoid the interaction with MPS and rapid clearance by RES, exhibiting the "stealth" state due to the masking of the TAT peptide during blood circulation. Once accumulated in the tumor tissues, the masked TAT peptide was reactivated by the tumor acidity, which induced ^{DA}TAT-NP$_{IR\&DOX}$ nanoparticles to transform into the "recognize" state, markedly promoting their interaction with tumor cells for enhanced cellular internalization. Then, these nanoparticles were transformed into "attack" state under NIR irradiation, achieving the supersensitive DOX release (Fig. 4). After systematically evaluating the effect of these transformable nanoparticles on their interaction with biological systems and overall therapeutic efficiency, they believed that this work provided a new avenue for the construction of the next generation of drug delivery systems. In addition, another kind of shell-sheddable nanoparticles that could deshield their PEG protective shell in the situation of tumor acidity was also reported by the same group[27, 29]. Similarly, amidization of the CPPs' lysine residues to succinyl amides showed efficient inhibition in their nonspecific interactions *in vivo*. Once the amides were hydrolyzed in an acidic environment, the CPPs' cell membrane penetration and nuclear localization activity were recovered[58]. Compared with cationic charge-shielding approaches, the amidized CPPs are very stable and have completely inhibited nonspecific interactions in the blood compartment.

Light is a cheap and easily manipulated clean external stimulus, whose variable wavelength and intensity can regulate the shape and size of the PAs at a desired time and place in a spatiotemporal precision manner. Light-responsive PAs have received increasing attention due to their potential applications in the diagnosis and treatment[59–65]. Most of the

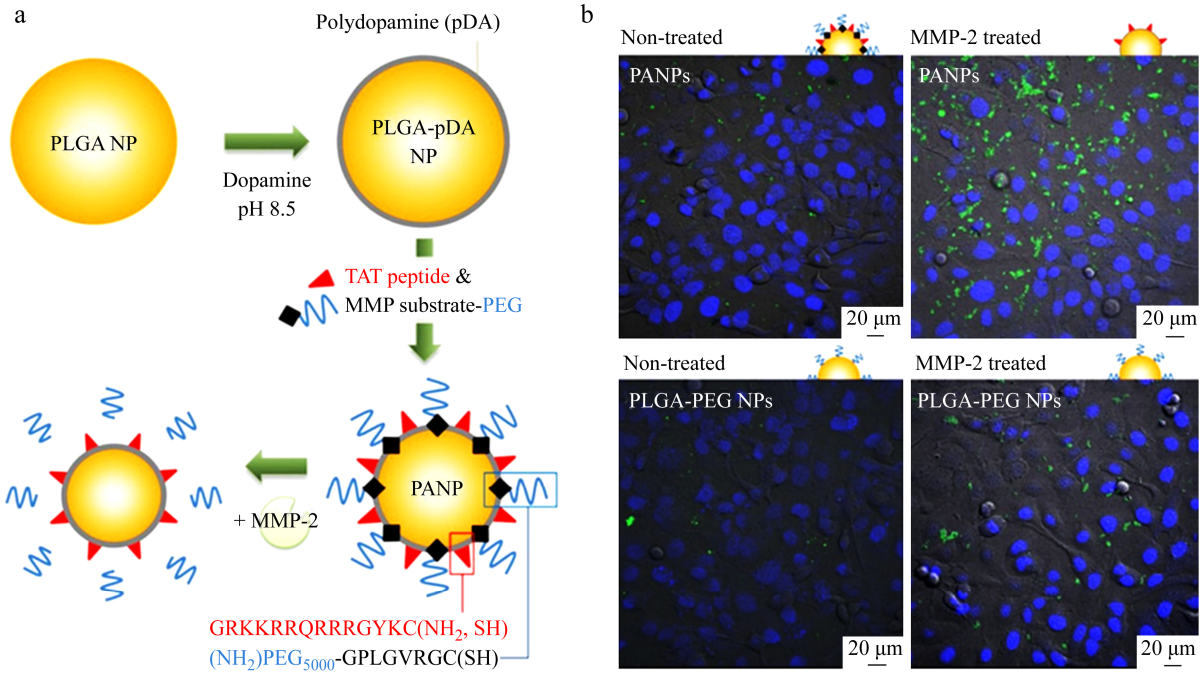


Fig. 3 (a) Schematic diagram of a peritumorally activatable nanoparticle (PANP); (b) Cellular uptake of NPs with or without MMP-2 pre-treatment (Reproduced with permission from Ref. [53]; Copyright (2013) Springer)

https://doi.org/10.1007/s10118-018-2035-9

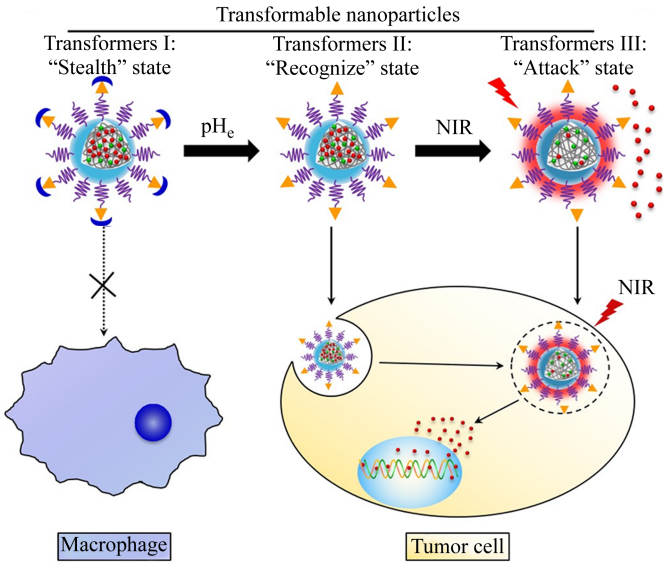


Fig. 4 Schematic illustration of tumor acidity/NIR controlled transformable nanoparticle ^{DA}TAT-NP$_{IR\&DOX}$ for mediating nanobio interaction from the injection site to biological targets (Reproduced with permission from Ref. [54]; Copyright (2017) American Chemical Society)

already reported examples were mainly concerning the light-triggered hydrophobicity-hydrophilicity transition or degradation of nanocarriers to induce drug release. Nowadays, photocaging, where a specific molecule or ligand is screened with a photolabile protecting group, will result in an inert caged molecule. Upon light irradiation, the caged molecule or ligand is exposed to the outside and becomes active. By using this elegant method, the species for light-controlled targeting have been constructed through the introduction of photocaging groups. For example, Dvir *et al*. caged GGGGYIGSR-NH_2 peptide with a 4,5-dimethoxy-2-nitrobenzyl (DMNB) group on tyrosine to form inactive GGGGY(DMNB)IGSR-NH_2 peptide. After illumination, the caging group could be released at the desired site and the targeting became active[66]. Moreover, Fan *et al.* reported a design of photocaged folate nanoconjugates bearing Au nanoparticles with caged folate molecules attached on the surface, which could selectively target cancer cells upon UV irradiation[67]. The FA was firstly masked by a photocleavable *o*-nitrobenzyl (ONB) moiety through covalent binding to α- and γ-carboxylate groups. Then, the light-activated targeting and intracellular drug delivery were demonstrated using biodegradable PLGA@lipid hybrid nanoparticles encapsulating the drug paclitaxel. The experimental results confirmed that the obtained hybrid nanoparticles showed a higher cytotoxicity to the target cells than the unactivated nanoparticles (Fig. 5).

FOR STEPS 4–5

As mentioned above, steps 1–3 concern the blood circulation and tumor accumulation and penetration of PAs. As soon as the cell endocytosis of PAs occurs, the encapsulated cargos, especially drugs, should require rapid release to play a set role on demand. In order to track and evaluate the release of drugs, visualization technology is particularly important. Thus, *in vivo* imaging has become a powerful tool to provide us with

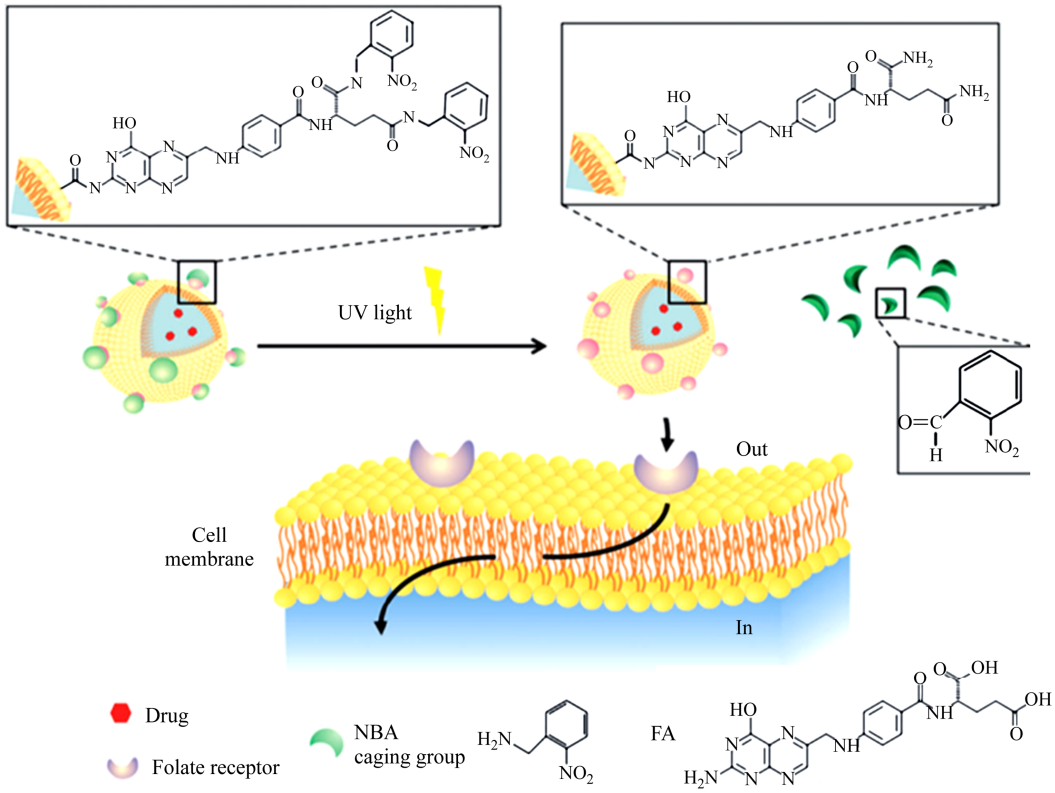


Fig. 5 The photocaged folate nanoconjugates activated by irradiation to remove the caging groups and then to target cancer cells (NBA = 2-nitrobenzylamine.) (Reproduced with permission from Ref. [67]; Copyright (2012) John Wiley and Sons)

https://doi.org/10.1007/s10118-018-2035-9

an in-depth high-resolution and high-contrast observation in living subjects and plays a pivotal role in the clinical accurate diagnostics of disease. In the past few years, fluorescence imaging, magnetic resonance imaging (MRI), photoacoustic imaging, computed tomography (CT), and radionuclide imaging have been developed in turn[68–72]. However, due to the urgent requirement of accurate *in situ* diagnosis and therapy, tumor and cell imaging technology guided treatment, namely theranostics, has become a newly presented research hotspot[73–77]. Encapsulating contrast agents together with drugs within single PAs can not only afford intelligent control over delivery but also increase the diagnostic sensitivity and specificity by means of multiplex modularity of design. The explosive growth in this field has led to a dizzying array of new nanocarriers, and many excellent works have been reported in the past decades. For example, Chen group encapsulated cyanine dyes, chemotherapeutic drugs, and photosensitizer within polymeric micelles or vesicles to form the complex theranostic platform. These systems not only possessed high drug payload efficiency but also achieved high-contrast fluorescence imaging-guided thermo-chemotherapy under pH and reduction responsive triggers or light irradiation, causing complete ablation of resistant tumor[78–81].

Despite the fact that many efforts have been made to design and optimize stimuli-responsive polymer based bioimaging and drug delivery system, more precise and innovative techniques need to be developed to adapt to the more complicated situations. For instance, most of the reported stimuli- responsive block copolymer delivery systems always perform a single imaging capability or responsive to a single stimulus to release drugs, which cannot fulfill the more complicated imaging, drug delivery and release needs. Development of multifunctional theranostic agent that integrates the advantages of multi-tier diagnosis and therapy into a single platform has been of great importance[82–84]. To meet this demand, a smart amphiphilic copolymer was prepared with poly(ε-caprolactone) (PCL) as hydrophobic block, PEGylated helical poly(phenyl isocyanide) (PPI) as hydrophilic block, and a pH-responsive rhodamine B (RhB) moiety located in the junction. After packaging IR780 and camptothecin (CPT) within the micelle cores through cosolvent self-assembly, the IR780/CPT@PPI(-RhB)-PCL complex micelles were successfully achieved (Fig. 6a)[85].

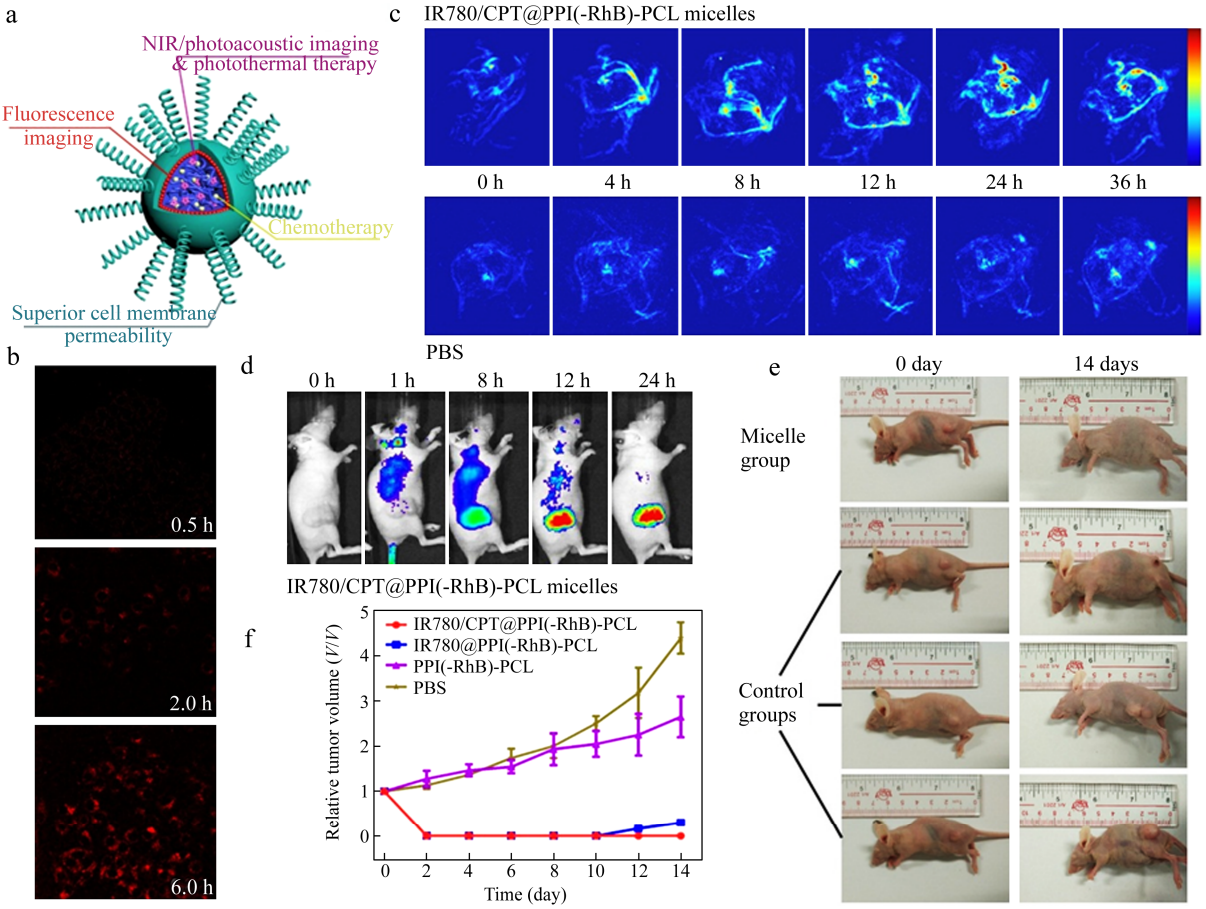


Fig. 6 (a) Schematic illustration of IR780/CPT@PPI(-RhB)-PCL complex micelles; (b) Incubation duration-dependent CLSM images of live HeLa cells when culturing at 37 °C with IR780/CPT@PPI(-RhB)-PCL complex micelles; Time-lapse (c) photoacoustic MAP and (d) NIR fluorescence (NIRF) images in mice taken at different time after intravenous injection of IR780/CPT@PPI(-RhB)-PCL complex micelles; (e) Effects of chemo-photothermal therapy in HeLa tumor-bearing mice (representative time-dependent photos taken for mice after being irradiated by 808 nm NIR light irradiation); (f) Tumor volumes of different groups measured after laser irradiation and normalized to their initial size (n = 5 per group) (Error bars indicated the means and standard errors.) (Reproduced with permission from Ref. [85]; Copyright (2016) Ivyspring International Publisher)

https://doi.org/10.1007/s10118-018-2035-9

The *in vitro* and *in vivo* experiments demonstrated that the pH-induced fluorescent responsiveness (Fig. 6b) and NIR-triggered strong acoustic and heat generation endowed them with efficient photoacoustic (Fig. 6c) and NIR-fluorescent (Fig. 6d) imaging capability for cancer diagnosis. Moreover, with NIR laser irradiation, the generated heat significantly improved the CPT release, leading to synergetic chemo-photothermal therapy (Fig. 6e) and decreased tumor recurrence rates in mice (Fig. 6f). Overall, the biocompatible multifunctional micelles with these combined advantages can potentially be utilized for multi-mode imaging guided disease diagnosis and therapy.

One more worthy work concerning a pH-, thermal-, and glutathione multi-responsive polymer zipper consisting of cell-penetrating poly(disulfide)s and thermosensitive poly(*N*-isopropylacrylamide)s bearing guanidinium/phosphate (Gu^+/pY^-) moieties to adjust the surface composition of nanocarriers for precise tumor targeting and efficient drug delivery is developed by Zhang *et al*[86]. The nanocarriers could remain in undetected state during blood circulation and favor passive accumulation at tumor sites. With the assistance of acidic microenvironment and NIR irradiation (photothermal conversion), the Gu^+/pY^- interaction was broken, leading to the rupture of zipper and exposing the penetrating shell (Fig. 7). The *in vivo* experiments confirmed that the nanocarriers showed longer blood circulation time, minimized uptake and drug leakage in normal organs, and enhanced accumulation and efficient drug release at tumor sites by manipulating the surface properties, which largely inhibited the tumor growth. This proof-of-concept provided a versatile protocol for engineering nanomedicines with high selectivity and efficiency for clinical cancer treatment.

However, it should be noted that, due to the thermodynamic equilibrium, conventional PAs may dissociate into unimers at a concentration lower than the critical micelle concentration (CMC) upon high dilution, such as intravenous injection, leading to premature release of encapsulated cargos, like contrast agent or drugs, before reaching the target tissues. This will result in reduced therapeutic efficacy and make the major contributor to cancer therapy turn out to be the shortcoming in imaging. To address this issue, the use of core cross-linked (CCL) micelles emerged as an effective approach bearing ionic interaction, photo-cross-linking, condensation, and "click" reactions[87–92]. On the contrary, in the case of drug delivery systems, the PAs must dissociate or swell to release entrapped drugs at the targeted site. Although we are committing to the perfect design, currently available PAs still have difficulties in fulfilling all of the application requirements. With the help of light-regulated "traceless" crosslinking strategy, Wang *et al.* gave a perfect solution of the long-standing dilemma of the synchronized stability and permeability of vesicles. An amphiphilic block copolymer with the hydrophilic PEO block and hydrophobic PNBOC block containing photolabile

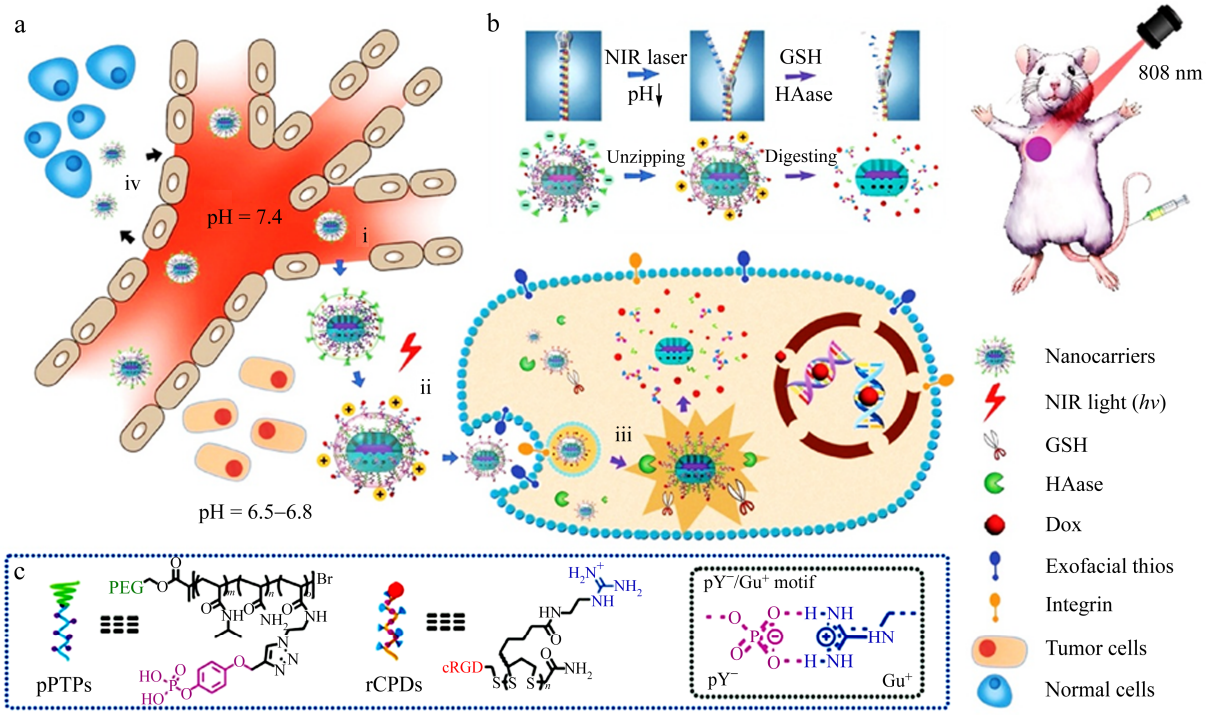


Fig. 7 Schematic design of smart nanocarriers coated with pH-/thermal-/GSH-responsive polymer zippers for precision tumor treatment: (a) NIR-/pH-guided cellular uptake and GSH/HAase-controlled release *in vivo* ((i) passive accumulation at tumor sites in the PEG state *via* the EPR effect; (ii) NIR-/pH-activated surface shift to the rCPD state for selective uptake *via* thiol-/receptor-mediated endocytosis; (iii) endosome escape and controlled release by endogenous GSH/HAase; (iv) nonspecific retention and clearance in normal tissues); (b) The surface state variations during drug delivery (the polymer zipper decoding and the sandwich protective shell degradation); (c) The composition of the pPTP/CPD polymer zipper with multiple pY^-/Gu^+ salt bridges (The rCPDs were prepared with a cyclic peptide with sequence of arginine-glycine-aspartic acid (RGD) as an initiator.) (Reproduced with permission from Ref. [86]; Copyright (2017) John Wiley and Sons)

https://doi.org/10.1007/s10118-018-2035-9

carbamate-caged primary amine moieties, termed as PEO-*b*-PNBOC, was synthesized[93]. After self-assembling into vesicles, the caged primary amine groups could be released by light-triggered self-immolative decaging process, resulting in a hydrophobicity to hydrophilicity transition of the bilayer of vesicles. Perfectly, at the same time, the free amine groups took part in the subsequent crosslinking by amidation reactions with adjacent ester bonds, leading to enhanced vesicle stability instead of vesicle-to-unimer transition (Fig. 8). Getting the help from this feature, light-regulated co-release of both hydrophobic and hydrophilic cargos and light-switchable biocatalysis of enzyme entrapped vesicle nanoreactors were successfully achieved. Moreover, PEO-*b*-PSPA diblock copolymers containing a unique carbamate linkage in the PSPA block were also prepared by the same group[94]. Upon self-assembly, spiropyran (SP) moieties within vesicle bilayers underwent reversible phototriggered isomerization between hydrophobic SP and zwitterionic merocyanine (MC) states. No matter in what form, the microstructures of vesicles were stabilized by multiple cooperative noncovalent interactions including hydrophobic interaction, hydrogen bonding, π-π stacking, and electrostatic interactions. The carbamate-incurred hydrogen bonding interactions in the sample were confirmed to be crucial for vesicle stabilization in the zwitterionic MC state, and the reversible phototriggered SP-MC transition was accompanied by membrane polarity and permeability switching from being impermeable to selectively permeable toward noncharged, charged, and zwitterionic small molecule species below critical molar masses. The photoswitchable spatiotemporal release of dyes within living HeLa cells was further demonstrated. After comparing these two works, the former "traceless" crosslinking process is irreversible and the bilayer cross-linking is unidirectional transition. Not only that, the photo-triggered release of 2-nitrosobenzaldehyde intermediates may further incur cytotoxicity issues. But the later design provides an excellent solution to this issue.

Moreover, since Luo *et al*. observed the unique optical properties termed as "aggregation-induced emission (AIE)", tetraphenylethene (TPE) has emerged and opened the door for a new direction for functional materials[95]. However, most of the existing reports focused on their AIE phenomenon and applied this feature in fluorescence cellular tracers or chemosensing[96–100]. Recently, three TPE- functionalized monomers and catalysts were synthesized by attaching TPE moieties to phenyl isocyanide and by post-modification strategy from TPE, respectively. It had been confirmed that the monomers (TPE-NC) and corresponding homopolymers, no matter linear or four-armed star-shaped, exhibited concentration and molecular weight dependent AIE behavior in pure organic solvents. Differently, TPE-NC monomers maintained AIE activity in THF/H_2O mixture, but the

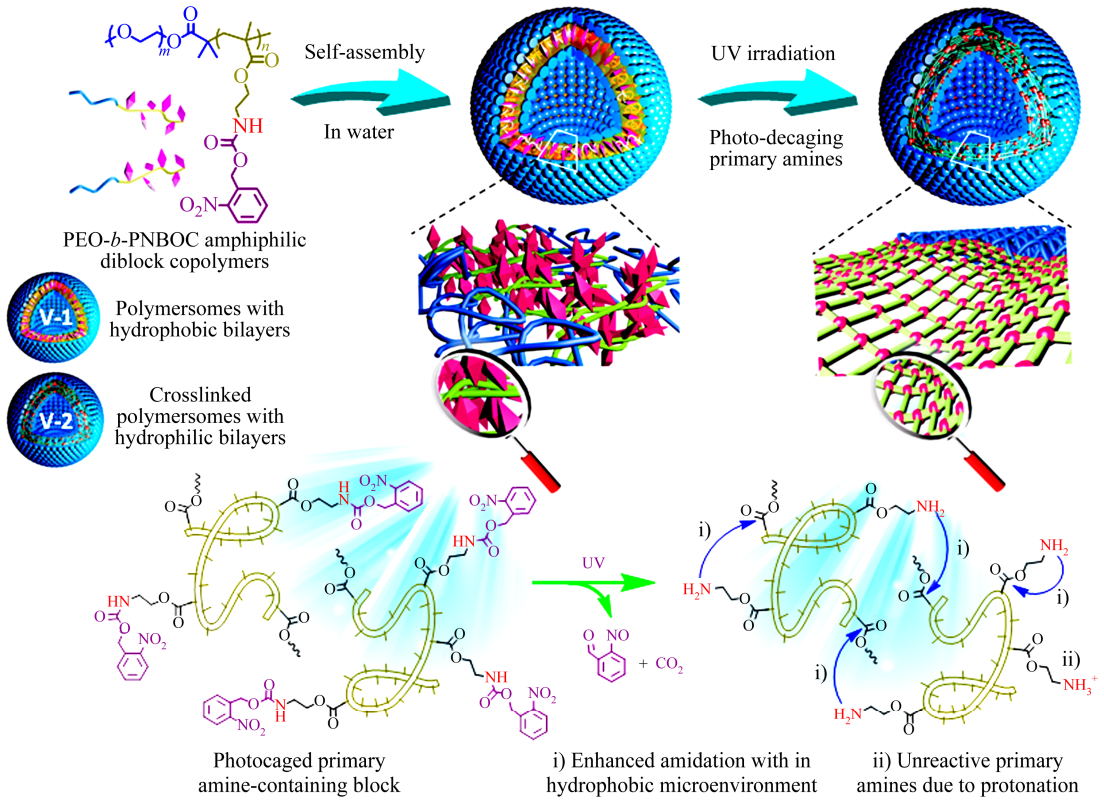


Fig. 8 Design of block copolymer vesicles exhibiting concurrent phototriggered "traceless" crosslinking and vesicle membrane permeabilization (PEO-*b*-PNBOC amphiphilic block copolymers self-assemble into polymersomes with the hydrophobic bilayer containing carbamate-caged primary amine moieties. UV irradiation triggers decaging reactions and the release of primary amine functionalities. Prominent amidation reaction then occurs because of a suppressed amine pK_a within the hydrophobic vesicle membrane, resulting in vesicle crosslinking instead of vesicle-to-unimer disassembly. i) Enhanced amidation within the hydrophobic microenvironment. ii) Unreactive primary amines because of protonation.) (Reproduced with permission from Ref. [93]; Copyright (2014) John Wiley and Sons)

https://doi.org/10.1007/s10118-018-2035-9

homopolymers lost their emission in mixed solvent. Thus, the aggregation-caused quenching (ACQ) behavior, a diametrically opposite phenomenon to AIE, from the same TPE moieties was observed[101]. Thanks to the continuous findings and designs, a new type of cross-linked cellular tracer and nanovectors with thiol ratiometric fluorescence imaging performance was reported by us[102]. Starting from three different kinds of phenyl isocyanide monomers, a type of well-defined amphiphilic block copolymers, P(PFPPI-*co*-TPEPI-*co*-HPPI)-*b*-HPPPI, with controlled molecular weights and tunable compositions were prepared through sequential living copolymerization in one pot (Fig. 9a). Disulfide bonds were then introduced by the exchange reaction between pentafluorophenol (PFP) units and cystamine (Cys; served as a cross-linker). The final cross-linked P(CysPI-*co*-TPEPI-*co*-HPPI)-*b*-HPPPI PAs (Fig. 9b) showed a time-dependent dissociation in the conditions mimicking the intracellular reducing environment, but became nonfluorescent (ACQ) if the polymer chains were aggregated. By taking advantage of this character, nanoassemblies capable of fluorescence ratiometric property could be constructed after incorporating another solvatochromic dyes, Nile red (NR), in water (Fig. 9c). In cells, the red fluorescence emission from NR channel observably decreased with time, but, at the same time, the blue fluorescence emission from TPE channel gradually increased in the same time scale (Fig. 9d). This change in the ratio of emission intensity (overlay column) showed a color transition from red to purple to blue, confirming the successful development of a polymeric assembly based ratiometric probes to realize the persistent and real-time cancer cell microenvironment responsive imaging even in the case of polymeric nanoassemblies' swelling induced cargo release. Not only that, these assemblies also possessed rapid cell membrane permeability due to the PEGylated single left-handed helical corona[103].

As mentioned above, although the structure of nanocarriers was stabilized through cross-linking method, the inevitable low drug loading efficiency still existed and tended to be a major obstacle to limit the therapy efficiency. In addition, a

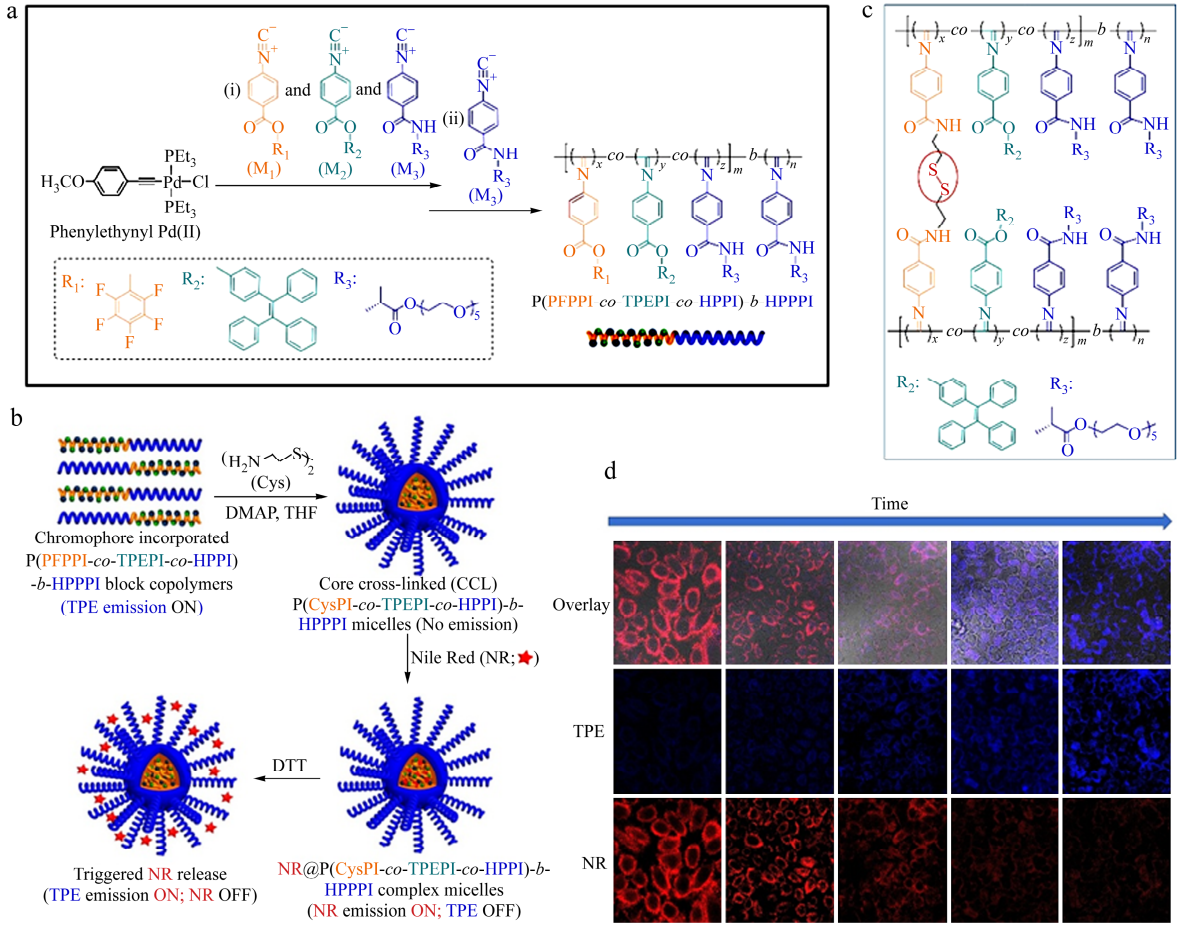


Fig. 9 (a) Synthetic routes employed for the successive copolymerization of pentafluorophenyl ester-functionalized phenyl isocyanide monomers (PFPPI; M_1), tetraphenylethene (TPE)-functionalized phenyl isocyanide monomers (TPEPI; M_2), and L-hydrophilic phenyl isocyanide monomers (HPPI; M_3) by living polymerization with phenylethynyl Pd(II) complex as a single catalyst to form P(PFPPI-*co*-TPEPI-*co*-HPPI)-*b*-HPPPI block copolymers in one-pot; (b) Schematic illustration for the fabrication of dye incorporated core cross-linked complex micelles and reducing agent-triggered release as well as their respective luminescence behaviour; (c) The chemical structure of resultant micelles; (d) Incubation duration-dependent CLSM images of live HeLa cells when culturing at 37 °C with NR@P(CysPI-*co*-TPEPI-*co*-HPPI)-*b*-HPPPI micelles at different time (Reproduced with permission from Ref. [102]; Copyright (2017) American Chemical Society)

https://doi.org/10.1007/s10118-018-2035-9

possibility of the mismatch between the releases of contrast agents and anticancer drugs from the PAs existed and might result in undesirable theranostic outcomes. To overcome this challenge, attaching drug molecules to the polymer chains to form "polymer-drug conjugates" and polymerizing prodrug monomers to form so-called "polyprodrugs" are two efficient implemented methods to improve the stability of encapsulated drugs[104, 105]. The introduction of stimuli-responsive linkage between drug molecules and polymer chains permits further precise control over drug release. For example, the preparation and relevant biological functions of an amphiphilic block copolymer, PEG-*b*-PCPTM, were reported by Hu *et al*[106]. The PCPTM block was obtained by polymerizing a reduction-cleavable CPT prodrug monomer, leading to the resultant diblock copolymer with a more than 50 wt% of CPT loading content, which was termed as "polyprodrug amphiphiles". The controlled hierarchical organization of polyprodrug amphiphiles as well as corresponding biological application was further investigated, and the unprecedented staggered lamellae assemblies outperform the other kinds of nanostructures. This work opens up new horizons for exploring block copolymer based drug delivery systems with improved drug loading efficacy and represents the typical example of polyprodrug amphiphiles, which are amenable to the investigation of biological performance. Based on this excogitation, a new class of theranostic nanoparticles constructed from hyperbranched polyprodrug amphiphiles consisting of reduction-activatable CPT prodrugs and Gd complex (MRI contrast agent) labelled hyperbranched, guanidine residue modified hydrophilic coronas was reported by the same group[107]. Upon cellular internalization, the accompanied turn-on of therapeutic potency and enhanced imaging ability in response to tumor milieu were achieved (Fig. 10). Such superior synergistic imaging and chemotherapy capability endowed the hyperbranched topology to be a valid candidate to design next-generation of theranostic polyprodrug platform. Similarly, a dimeric drug conjugate bearing a trigger responsive domain was designed by Cai *et al*[108]. Specifically, the CPT drug molecules were covalently conjugated to the 2,6-bis(hydroxymethyl)-aniline *via* carbonate linkages. Upon triggering, cleavage of the disulfide bond resulted in decomposition of the drug dimer, leading to the CPT release in their authentic form. This distinct structure not only prevented the formation of large drug aggregates, but also largely enhanced the drug loading content.

CONCLUSIONS AND PERSPECTIVES

Since polymer synthesis and nanoassembly technology experienced rapid development, stimuli-responsive block copolymers and corresponding PAs have emerged one after

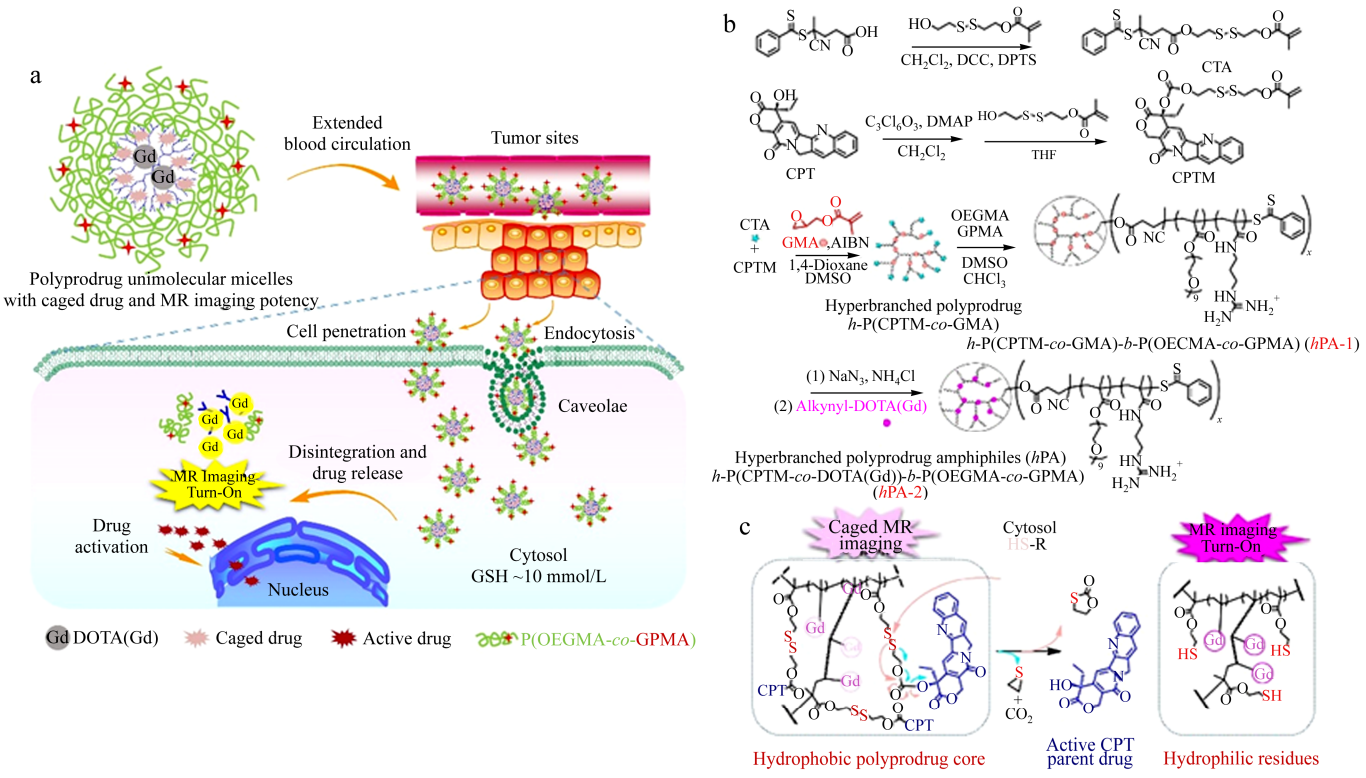


Fig. 10 (a) Schematic illustration of polyprodrug unimolecular micelles with hyperbranched cores conjugated with DOTA(Gd) and reductive milieu-cleavable camptothecin prodrugs and hydrophilic coronas functionalized with guanidine residues; (b) Reaction schemes employed for the synthesis of hyperbranched polyprodrug amphiphiles, *h*-P(CPTM-*co*-DOTA(Gd))-*b*-P(OEGMA-*co*-GPMA) (*h*PA-2); (c) Proposed mechanism of reductively activated CPT drug release in cytosol milieu from hyperbranched polyprodrug cores and concurrent hydrophobic-hydrophilic transition of the local milieu surrounding the Gd complex (Reproduced with permission from Ref. [107]; Copyright (2014) American Chemical Society)

https://doi.org/10.1007/s10118-018-2035-9

another. One of the most important outstanding features of these PAs is their utilization in targeted drugs and contrast agents delivery to tumor sites and performed stimuli-triggered controlled drug release and high resolution imaging. In this feature article, the newly emerging surface property engineering of tumor microenvironment responsive PAs with diverse structures and functions have been discussed, which integrated the extended blood circulation time and enhanced drug delivery in a single platform. Several methods, including PEGylation and dePEGylation (shell-sheddable), surface charge reversal, size transition of PAs, shielding and exposing targeting ligand or peptide were used to achieve the stealthy-to-sticky transition of PAs. These intelligent PAs are stealthy during blood circulation after intravenous injection, but the shielding matrices are removed by extracellular milieu stimuli (such as weak acidic pH, over-expressed enzymes, and redox species) or exogenous excitations (*e.g.*, light) when they reach tumor tissue.

Moreover, the dilemma of synchronized stability and permeability of PAs based drug delivery system has troubled the scholars in related fields for a long time. Fortunately, thanks to the light-regulated "traceless" crosslinking strategy, this problem has been satisfactorily resolved. Not only that, the concept of "polyprodrug amphiphiles" and multi-responsive theranostic platform open up new directions for exploring polymer based drug delivery systems with improved drug loading efficacy and imaging-guided cancer therapy.

Finally, considering the superior interactions with cell membranes, positively charged CPPs with a large number of arginine residues and their analogues (*e.g.*, guanidine-decorated copolymers) are performed as an efficient medium to facilitate cell internalization. It has been confirmed that the unique helical structure of CPPs is essential for their membrane interactions and promoting their cellular uptake[109–111]. Some CPPs mimics, such as positively charged helical poly(arginine)s and poly(disulfide)s[112, 113], were already synthesized which showed superior cell membrane permeability up to two orders of magnitude higher than that of TAT peptides. Inspired by this point, the artificial polymeric mimic exhibiting cell-penetrating properties is a very promising direction. Since the discovery of helical structures in biomacromolecules, artificial helical polymers with stable helical conformation in solution and in solid state have attracted considerable increasing attention. Up to now, several helical polymers, including polyisocyanate[114, 115], polyguanidines[116, 117], poly(phenyl isocyanide)[118–122], and polyisocyanides[123–125] have been synthesized and reported to be utilized in many areas. Therefore, we envision that functionalized artificial helical polymer chains that have a structural similarity to CPPs may also facilitate intracellular delivery of cargos and create a novel type of helical polymer-based delivery system.

ACKNOWLEDGMENTS

This work was financially supported by the National Natural Science Foundation of China (No. 51673058).

REFERENCES

1 Ross, J. S.; Schenkein, D. P.; Pietrusko, R.; Rolfe, M.; Linette, G. P.; Stec, J.; Stagliano, N. E.; Ginsburg, G. S.; Symmans, W. F.; Pusztai, L.; Hortobagyi, G. N. Targeted therapies for cancer. Am. J. Clin. Pathol. 2004, 122(4), 598–609.
2 Langer, R.; Tirrell, D. A. Designing materials for biology and medicine. Nature 2004, 428, 487–492.
3 Hu, J. M.; Liu, S. Y. Engineering responsive polymer building blocks with host-guest molecular recognition for functional applications. Acc. Chem. Res. 2014, 47(7), 2084–2095.
4 Yin, J.; Hu, H. B.; Wu, Y. H.; Liu, S. Y. Thermo- and light-regulated fluorescence resonance energy transfer processes within dually responsive microgels. Polym. Chem. 2011, 2, 363–371.
5 Hu, J. M.; Liu, S. Y. Recent advances towards the fabrication and biomedical applications of responsive polymeric assemblies and nanoparticle hybrid superstructures. Dalton Trans. 2015, 44, 3904–3922.
6 Yin, J.; Chen, Y.; Zhang, Z. H.; Han, X. Stimuli-responsive block copolymer-based assemblies for cargo delivery and theranostic applications. Polymers 2016, 8(7), 268–296.
7 Zheng, X. C.; Wang, X.; Mao, H.; Wu, W.; Liu, B. R.; Jiang, X. Q. Hypoxia-specific ultrasensitive detection of tumours and cancer cells *in vivo*. Nat. Commun. 2015, 6, DOI: 10.1038/ncomms6834
8 Yin, J.; Hu, J. M.; Zhang, G. Y.; Liu, S. Y. Schizophrenic core-shell microgels: thermoregulated core and shell swelling/collapse by combining ucst and lcst phase transitions. Langmuir 2014, 30(9), 2551–2558.
9 Zheng, X. C.; Mai, H.; Huo, D.; Wu, W.; Liu, B. R.; Jiang, X. Q. Successively activatable ultrasensitive probe for imaging tumour acidity and hypoxia. Nat. Biomed. Eng. 2017, 1, DOI: 10.1038/s41551-017-0057
10 Yin, J.; He, Y. G.; Li, W.; Wu, Z. Q.; Ding, Y. S. Wide range temperature detection with hybrid nanoparticles traced by surface-enhanced Raman scattering. Sci. China Chem. 2014, 57(3), 417–425.
11 Zhang, L. Z.; Zhang, Y. J.; Wu, W.; Jiang, X. Q. Doxorubicin-loaded boron-rich polymer nanoparticles for orthotopically implanted liver tumor treatment. Chinese J. Polym. Sci. 2013, 31(5), 778–786.
12 Long, C. Y.; Sheng, M. M.; He, B.; Wu, Y.; Wang, G.; Gu, Z. W. Comparison of drug delivery properties of PEG-*b*-PDHPC micelles with different compositions. Chinese J. Polym. Sci. 2012, 30(3), 387–396.
13 Lu, Y.; Aimetti, A. A.; Langer, R.; Gu, Z. Bioresponsive materials. Nat. Rev. Mater. 2017, 2(1), 16075.
14 Hu, J. M.; Zhang, G. Q.; Liu, S. Y. Enzyme-responsive polymeric assemblies, nanoparticles and hydrogels. Chem. Soc. Rev. 2012, 41, 5933–5949.
15 Yin, J.; Shi, S. Y.; Hu, J. M.; Liu, S. Y. Construction of polyelectrolyte-responsive microgels, and polyelectrolyte concentration and chain length-dependent adsorption kinetics. Langmuir 2014, 30(31), 9551–9559.
16 Wu, Y. Z.; Zhang, Z. H.; Han, X.; Zhang, J.; Zhang, W. M.; Yin, J. Affinity switching for lysozyme and dual-responsive microgels by stopped-flow technique: kinetic control and activity evaluation. Chinese J. Polym. Sci. 2017, 35(8), 950–960.
17 Deng, Z. Y.; Hu, J. M.; Liu, S. Y. Reactive oxygen, nitrogen, and sulfur species (RONSS)-responsive polymersomes for triggered drug release. Macromol. Rapid Commun. 2017, 38(11), DOI: 10.1002/marc.201600685

18 Ge, Z. S.; Liu, S. Y. Functional block copolymer assemblies responsive to tumor and intracellular microenvironments for site-specific drug delivery and enhanced imaging performance. Chem. Soc. Rev. 2013, 42, 7289–7325.
19 Barenholz, Y. Doxil®-The first FDA-approved nano-drug: lessons learned. J. Control. Release 2012, 160, 117–134.
20 Von Hoff, D. D.; Ramanathan, R. K.; Borad, M. J.; Laheru, D. A.; Smith, L. S.; Wood, T. E.; Korn, R. L.; Desai, N.; Trieu, V.; Iglesias J. L.; Zhang, H.; Soon-Shiong, P.; Shi, T.; Rajeshkumar, N. V.; Maitra, A; Hidalgo, M. J. Gemcitabine plus nab-paclitaxel is an active regimen in patients with advanced pancreatic cancer: a phase I/II trial. Clin. Oncol. 2011, 29(34), 4548–4554.
21 Forssen, E. A. The design and development of DaunoXome® for solid tumor targeting *in vivo*. Adv. Drug Delivery Rev. 1997, 24, 133–150.
22 Bregoli, L.; Movia, D.; Gavigan-Imedio, J. D.; Lysaght, J.; Reynolds, J.; Prina-Mello, A. Nanomedicine applied to translational oncology: a future perspective on cancer treatment. Nanomed. Nanotechnol. Biol. Med. 2016, 12, 81–103.
23 Sun, Q.; Zhou, Z.; Qiu, N.; Shen, Y. Rational design of cancer nanomedicine: nanoproperty integration and synchronization. Adv. Mater. 2017, 29(14), DOI: 10.1002/adma.201606628
24 Sun, Q.; Radosz, M.; Shen, Y. J. Challenges in design of translational nanocarriers. J. Control. Release 2012, 164, 156–169.
25 Otsuka, H.; Nagasaki, Y.; Kataoka, K. PEGylated nanoparticles for biological and pharmaceutical applications. Adv. Drug Delivery Rev. 2003, 55, 403–419.
26 Talelli, M.; Rijcken, C. J. F.; Van, N. C. F.; Storm, G.; Hennink, W. E. Micelles based on HPMA copolymers. Adv. Drug Delivery Rev. 2010, 62, 231–239.
27 Sun, C.Y.; Shen, S.; Xu, C. F.; Li, H. J.; Liu, Y.; Cao, Z. T.; Yang, X. Z.; Xia, J. X.; Wang, J. Tumor acidity-sensitive polymeric vector for active targeted siRNA delivery. J. Am. Chem. Soc. 2015, 137(48), 15217–15224.
28 Sethuraman, V. A.; Na, K.; Bae, Y. H. pH-Responsive sulfonamide/PEI system for tumor specific gene delivery: an *in vitro* study. Biomacromolecules 2006, 7(1), 64–70.
29 Zhu, L.; Wang, T.; Perche, F.; Taigind, A.; Torchilin, V. P. Enhanced anticancer activity of nanopreparation containing an MMP2-sensitive PEG-drug conjugate and cell-penetrating moiety. Proc. Natl. Acad. Sci. USA 2013, 110(42), 17047–17052.
30 Yang, X. Z.; Du, J. Z.; Dou, S.; Mao, C. Q.; Long, H. Y.; Wang, J. Sheddable ternary nanoparticles for tumor acidity-targeted siRNA delivery. ACS Nano 2012, 6(1), 771–781.
31 Sun, C. Y.; Liu, Y.; Du, J. Z.; Cao, Z. T.; Xu, C. F.; Wang, J. Facile generation of tumor-pH-Labile linkage-bridged block copolymers for chemotherapeutic delivery. Angew. Chem. Int. Ed. 2016, 55(3), 1010–1014.
32 Chen, J. J.; Ding, J. X.; Xiao, C. S.; Zhuang, X. L.; Chen, X. S. Emerging antitumor applications of extracellularly reengineered polymeric nanocarriers. Biomater. Sci. 2015, 3, 988–1001.
33 Liu, J. J.; Chen, Q.; Zhu, W. W.; Yi, X.; Yang, Y.; Dong, Z. L.; Liu, Z. Nanoscale-coordination-polymer-shelled manganese dioxide composite nanoparticles: a multistage Redox/pH/H_2O_2-responsive cancer theranostic nanoplatform. Adv. Funct. Mater. 2017, 27(10), 1605926(1-11).
34 Torchilin, V. P. TAT peptide-mediated intracellular delivery of pharmaceutical nanocarriers. Adv. Drug Delivery Rev. 2008, 60, 548–558.
35 Wang, W. W.; Cheng, D.; Gong, F. M.; Miao, X. M.; Shuai, X. T. Design of multifunctional micelle for tumor-targeted intracellular drug release and fluorescent imaging. Adv. Mater. 2012, 24(1), 115–120.
36 Remant, B. K. C.; Chandrashekaran, V.; Cheng, B.; Chen, H.; Peña, M. M. O.; Zhang, J.; Montgomery, J.; Xu, P. S. Redox potential ultrasensitive nanoparticle for the targeted delivery of camptothecin to HER2-positive cancer cells. Mol. Pharm. 2014, 11(6), 1897–1905.
37 Xu, P.; van Kirk, E. A.; Zhan, Y.; Murdoch, W. J.; Radosz, M.; Shen, Y. Targeted charge-reversal nanoparticles for nuclear drug delivery. Angew. Chem. Int. Ed. 2007, 46(26), 4999–5002.
38 Du, J. Z.; Du, X. J.; Mao, C. Q.; Wang J. Tailor-made dual ph-sensitive polymer-doxorubicin nanoparticles for efficient anticancer drug delivery. J. Am. Chem. Soc. 2011, 133(44), 17560–17563.
39 Han, S. S.; Li, Z. Y.; Zhu, J. Y.; Han, K.; Zeng, Z. Y.; Hong, W.; Li, W. X.; Jia, H. Z.; Liu, Y.; Zhuo, R. X. Dual-pH sensitive charge-reversal polypeptide micelles for tumor-triggered targeting uptake and nuclear drug delivery. Small 2015, 11(21), 2543–2554.
40 Sui, M. H.; Liu, W. W.; Shen, Y. Q. Nuclear drug delivery for cancer chemotherapy. J. Control. Release 2011, 155, 227–236.
41 Wang, N.; Dong, A. J.; Tang, H. D.; van Kirk, E. A.; Johnson, P. A.; Murdoch, W. J.; Radosz, M.; Shen, Y. Q. Synthesis of degradable functional poly(ethylene glycol) analogs as versatile drug delivery carriers. Macromol. Biosci. 2007, 7(11), 1187–1198.
42 Sethuraman1, V. A.; Bae, Y. H. TAT peptide-based micelle system for potential active targeting of anti-cancer agents to acidic solid tumors. J. Control. Release 2007, 118, 216–224.
43 Zhang, Y.; Wang, X. J.; Guo, M.; Yan, H. S.; Wang, C. H.; Liu, K. L. Cisplatin-loaded polymer/magnetite composite nanoparticles as multifunctional therapeutic nanomedicine. Chinese J. Polym. Sci. 2014, 32(10), 1329–1337.
44 Yuan, F.; Dellian, M.; Fukumura, D.; Leunig, M.; Berk, D. A.; Torchilin, V. P.; Jain, R. K. Vascular permeability in a human tumor xenograft: molecular size dependence and cutoff size. Cancer Res. 1995, 55(17), 3752–3756.
45 Cabral, H.; Matsumoto, Y.; Mizuno, K.; Chen, Q.; Murakami, M.; Kimura, M.; Terada, Y.; Kano, M. R.; Miyazono, K.; Uesaka, M.; Nishiyama, N.; Kataoka, K. Accumulation of sub-100 nm polymeric micelles in poorly permeable tumours depends on size. Nat. Nanotechnol. 2011, 6, 815–823.
46 Chauhan, V. P.; Stylianopoulos, T.; Martin, J. D.; Popovic, Z.; Chen, O.; Kamoun, W. S.; Bawendi, M. G.; Fukumura, D.; Jain, R. K. Normalization of tumour blood vessels improves the delivery of nanomedicines in a size-dependent manner. Nat. Nanotechnol. 2012, 7, 383–388.
47 Sun, Q. H.; Sun, X. R.; Ma, X.P.; Zhou, Z. X.; Jin, E. L.; Zhang, B.; Shen, Y. Q.; van Kirk, E.; Murdoch, W. J.; Lott, J. P.; Lodge, T. P.; Radosz, M.; Zhao, Y. L. Integration of nanoassembly functions for an effective delivery cascade for cancer drugs. Adv. Mater. 2014, 26(45), 7615–7621.
48 Piedrafita, G.; Keller, M. A.; Ralser, M. The impact of non-enzymatic reactions and enzyme promiscuity on cellular metabolism during (oxidative) stress conditions. Biomolecules 2015, 5(3), 2101–2122.
49 Ghadiali, J. E.; Stevens, M. M. Enzyme-responsive nanoparticle systems. Adv. Mater. 2008, 20(22), 4359–4363.
50 Hahn, M. E.; Gianneschi, N. C. Enzyme-directed assembly and manipulation of organic nanomaterials. Chem. Commun. 2011, 47, 11814–11821.
51 Ulijn, R. V. Enzyme-responsive materials: a new class of smart biomaterials. J. Mater. Chem. 2006, 16, 2217–2225.
52 Li, Y. M.; Liu, G. H.; Wang, X. R;, Hu, J. M.; Liu, S. Y. Enzyme-responsive polymeric vesicles for bacterial-

strain-selective delivery of antimicrobial agents. Angew. Chem. Int. Ed. 2016, 55(5), 1760–1764.
53 Gullotti, E.; Park, J.; Yeo, Y. Polydopamine-based surface modification for the development of peritumorally activatable nanoparticles. Pharm. Res. 2013, 30(8), 1956–1967.
54 Li, D. D.; Ma, Y. C.; Du, J. Z.; Tao, W.; Du, X. J.; Yang, X. Z.; Wang, J. Tumor acidity/NIR controlled interaction of transformable nanoparticle with biological systems for cancer therapy. Nano Lett. 2017, 17(5), 2871–2878.
55 Jin, E. L.; Zhang, B.; Sun, X. R.; Zhou, Z. X.; Ma, X. P.; Sun, Q. H.; Tang, J. B.; Shen, Y. Q.; Van Kirk, E.; Murdoch, W. J.; Radosz, M. Acid-active cell-penetrating peptides for *in vivo* tumor-targeted drug delivery. J. Am. Chem. Soc. 2013, 135(2), 933–940.
56 Li, Y. M.; Yang, J. H.; Xu, B.; Gao, F.; Wang, W.; Liu, W. G. Enhanced therapeutic siRNA to tumor cells by a pH-sensitive agmatine-chitosan bioconjugate. ACS Appl. Mater. Interfaces 2015, 7(5), 8114–8124.
57 Huang, S. X.; Shao, K.; Liu, Y.; Kuang, Y. Y.; Li, J. F.; An, S.; Guo, Y. B.; Ma, H. J.; Jiang, C. Tumor-targeting and microenvironment-responsive smart nanoparticles for combination therapy of antiangiogenesis and apoptosis. ACS Nano 2013, 7(3), 2860–2871.
58 Jin, E. L.; Zhang, B.; Sun, X. R.; Zhou, Z. X.; Ma, X. P.; Sun, Q. H.; Tang, J. B.; Shen, Y. Q.; Kirk, E. V.; Murdoch, W. J.; Radosz, M. Acid-active cell-penetrating peptides for *in vivo* tumor-targeted drug delivery. J. Am. Chem. Soc. 2013, 135(2), 933–940.
59 Xia, D. Y.; Yu, G. C.; Li, J. Y.; Huang, F. H. Photo-responsive self-assembly based on a water-soluble pillar[6]arene and an azobenzene-containing amphiphile in water. Chem. Commun. 2014, 50, 3606–3608.
60 Xia, D. Y.; Wei, P. F.; Shi, B. B.; Huang, F. H. A pillar[6]arene-based [2]pseudorotaxane in solution and in the solid state and its photo-responsive self-assembly behavior in solution. Chem. Commun. 2016, 52, 513–516.
61 Zhao, Y. Light-responsive block copolymer micelles. Macromolecules 2012, 45(9), 3647–3657.
62 Li, Y. M.; Qian, Y. F.; Liu, T.; Zhang, G. Y.; Liu, S. Y. Light-triggered concomitant enhancement of magnetic resonance imaging contrast performance and drug release rate of functionalized amphiphilic diblock copolymer micelles. Biomacromolecules 2012, 13(11), 3877–2886.
63 Karimi, M.; Zangabad, P. S.; Baghaee-Ravari, S.; Ghazadeh, M.; Mirshekari, H.; Hamblin, M. R. Smart nanostructures for cargo delivery: uncaging and activating by light. J. Am. Chem. Soc. 2017, 139(13), 4584–4610.
64 Hu, J. J.; Chen, Y. H.; Li, Y. Q.; Zhou, Z. G.; Cheng, Y. Y. A thermo-degradable hydrogel with light-tunable degradation and drug release. Biomaterials 2017, 112, 133–140.
65 Chen, Q.; Xu, L. G.; Liang, C.; Wang, C.; Peng, R.; Liu, Z. Photothermal therapy with immune-adjuvant nanoparticles together with checkpoint blockade for effective cancer immunotherapy. Nat. Commum. 2016, 7, DOI: 10.1038/ncomms13193
66 Dvir, T.; Banghart, M. R.; Timko, B. P.; Langer, R.; Kohane, D. S. Photo-targeted nanoparticles. Nano Lett. 2010, 10(1), 250–254.
67 Fan, N. C.; Cheng, F. Y.; Ho, J. A.; Yeh, C. S. Photocontrolled targeted drug delivery: photocaged biologically active folic acid as a light-responsive tumor-targeting molecule. Angew. Chem. Int. Ed. 2012, 51(35), 8806–8810.
68 Cui, D.; Xie, C.; Pu, C. Y. Development of semiconducting polymer nanoparticles for photoacoustic imaging. Macromol. Rapid Commun. 2017, 38(12), DOI: 10.1002/marc.201700125
69 Hong, B. J.; Swindell, E. P.; MacRenaris, K. W.; Hankins. P. L.; Chipre, A, J.; Mastarone, D.; Ahn R. W.; Meade, T. J.; O'Halloran, T. V.; Nguyen, S. T. pH-responsive theranostic polymer-caged nanobins: enhanced cytotoxicity and T1 MRI contrast by HER2 targeting. Part. Syst. Charact. 2013, 30(9), 770–774.
70 Li, B. A novel upconversion nanotheranostic agent for multi-modality imaging-guided chemotherapy with on-demand drug release. Sci. China Chem. 2015, 58(6), 970–70.
71 Langer, A. A systematic review of PET and PET/CT in oncology: a way to personalize cancer treatment in a cost-effective manner? BMC Health Serv. Res. 2010, 10, DOI: 10.1186/1472-6963-10-283
72 Ke, C. Y.; Mathias, C. J.; Green, M. A. Folate-receptor-targeted radionuclide imaging agents. Adv. Drug Delivery Rev. 2004, 56, 1143–1160.
73 Smith, B. R.; Gambhir, S. S. Nanomaterials for *in vivo* imaging. Chem. Rev. 2017, 117(3), 901–986.
74 Ma, Y. F.; Huang, J.; Song, S. J.; Chen, H. B.; Zhang, Z. J. Cancer-targeted nanotheranostics: recent advances and perspectives. Small 2016, 12(36), 4936–4954.
75 Li, X. S.; Kim, J. H.; Yoon, J. Y.; Chen, X. Y. Cancer-associated, stimuli-driven, turn on theranostics for multimodality imaging and therapy. Adv. Mater. 2017, 29(23), 1606857(1-24).
76 Wang, S.; Huang, P.; Chen, X. Y. Stimuli-responsive programmed specific targeting in nanomedicine. ACS Nano 2016, 10(3), 2991–2994.
77 Deng, J.; Gao, C. Y. Recent advances in interactions of designed nanoparticles and cells with respect to cellular uptake, intracellular fate, degradation and cytotoxicity. Nanotechnology 2016, 27(41), 412002.
78 Guo, M.; Mao, H. J.; Li, Y. L.; Zhu, A. J.; He, H.; Yang, H.; Wang, Y. Y.; Tian, X.; Ge, C. C.; Peng, Q. L.; Wang, X. Y.; Yang, X. L.; Chen, X. Y.; Liu, G.; Chen, H. B. Dual imaging-guided photothermal/photodynamic therapy using micelles. Biomaterials 2014 , 35, 4656–4666.
79 Wan, Z. H.; Mao, H. J.; Guo, M.; Li, Y. L.; Zhu, A. J.; Yang, H.; He, H.; Shen, J. K.; Zhou, L. J.; Jiang, Z.; Ge, C. C.; Chen, X. Y.; Yang, X. L.; Liu, G.; Chen, H. B. Highly efficient hierarchical micelles integrating photothermal therapy and singlet oxygen-synergized chemotherapy for cancer eradication. Theranostics 2014, 4(4), 399–411.
80 Li, Y.; Deng, Y.; Tian, X.; Ke, H.; Guo, M.; Zhu, A. J.; Yang, T.; Guo, Z. Q.; Ge, Z. S.; Yang, X. L.; Chen, H. B. Multipronged design of light-triggered nanoparticles to overcome cisplatin resistance for efficient ablation of resistant tumor. ACS Nano 2015, 9(10), 9626–9637.
81 Zhu, A. J.; Miao, K.; Deng, Y. B.; Ke, H. T.; He, H.; Yang, T.; Guo, M.; Li, Y. L.; Guo, Z. Q.; Wang, Y. Y.; Yang, X. L.; Zhao, Y. L.; Chen, H. B. Dually pH/reduction-responsive vesicles for ultrahigh-contrast fluorescence imaging and thermo-chemotherapy-synergized tumor ablation. ACS Nano 2015, 9(8), 7874–7885.
82 Liu, G. H.; Wang, X. R.; Hu, J. M.; Zhang, G. Y.; Liu, S. Y. Self-immolative polymersomes for high-efficiency triggered release and programmed enzymatic reactions. J. Am. Chem. Soc. 2014, 136(20), 7492–7497.
83 Liu, G. H.; Zhang, G. F.; Hu, J. M.; Wang, X. R.; Zhu, M. Q.; Liu, S. Y. Hyperbranched self-immolative polymers (hSIPs) for programmed payload delivery and ultrasensitive detection. J. Am. Chem. Soc. 2015, 137(36), 11645–11655.
84 Frogley, B. J.; Wright, L. J. Cover picture: a metallaanthracene

and derived metallaanthraquinone. Angew. Chem. Int. Ed. 2017, 56(1), 143–147.
85 Shi, S. Y.; Liu, Y. J.; Chen, Y.; Zhang, Z. H.; Ding, Y. S.; Wu, Z. Q.; Yin, J.; Nie, L. M. Versatile pH-response micelles with high cell-penetrating helical diblock copolymers for photoacoustic imaging guided synergistic chemo-photothermal therapy. Theranostics 2016, 6(12), 2170–2182.
86 Zhang, P. H.; Wang, Y.; Lian, J.; Shen, Q.; Wang, C.; Ma, B.; Zhang, Y. C.; Xu, T. T.; Li, J. X.; Shao, Y. P.; Xu, F.; Zhu, J. J. Engineering the surface of smart nanocarriers using a pH-/thermal-/GSH-responsive polymer zipper for precise tumor targeting therapy *in vivo*. Adv. Mater. 2017, 29, 1702311.
87 Kakizawa, Y.; Harada, A.; Kataoka, K. Environment-sensitive stabilization of core-shell structured polyion complex micelle by reversible cross-linking of the core through disulfide bond. J. Am. Chem. Soc. 1999, 121(48), 11247–11248.
88 Wu, Z.; Huang, J. B.; Yan, Y. Electrostatic polyion micelles with fluorescence and MRI dual functions. Langmuir 2015, 31(29), 7926–7933.
89 Huynh, V. T.; Chen, G. J.; De, S. P.; Stenzel, M. H. Thiol-yne and Thiol-ene "click" chemistry as a tool for a variety of platinum drug delivery carriers, from statistical copolymers to crosslinked micelles. Biomacromolecules 2011, 12(5), 1738–1751.
90 O'Reilly, R. K.; Joralemon, M. J.; Hawker, C. J.; Wooley, K. L. Preparation of orthogonally-functionalized core Click cross-linked nanoparticles. New J. Chem. 2007, 31, 718–724.
91 Zhang, Z. H.; Yin, L. C.; Tu, C. L.; Song, Z. Y.; Zhang, Y. F.; Xu, Y. X.; Tong, R.; Zhou, Q.; Ren, J.; Cheng, J. J. Redox-responsive, core cross-linked polyester micelles. ACS Macro. Lett. 2013, 2(1), 40–44.
92 Deng, Z. Y.; Qian, Y. F.; Yu, Y. Q.; Liu, G. H.; Hu, J. M.; Zhang, G. Y.; Liu, S. Y. Engineering intracellular delivery nanocarriers and nanoreactors from oxidation-responsive polymersomes *via* synchronized bilayer cross-linking and permeabilizing inside live cells. J. Am. Chem. Soc. 2016, 138(33), 10452–10466.
93 Wang, X. R.; Liu, G. H.; Hu, J. M.; Zhang, G. Y.; Liu, S. Y. Concurrent block copolymer polymersome stabilization and bilayer permeabilization by stimuli-regulated "traceless" crosslinking. Angew. Chem. lnt. Ed. 2014, 53(12), 3138–3142.
94 Wang, X. R.; Hu, J. M.; Liu, G. H.; Tian, J.; Wang, H. J.; Gong, M.; Liu, S. Y.; Reversibly switching bilayer permeability and release modules of photochromic polymersomes stabilized by cooperative noncovalent interactions. J. Am. Chem. Soc. 2015, 137(48), 15262–15275.
95 Luo, J. D.; Xie, Z. L.; Lam, J. W. Y.; Cheng, L.; Chen, H. Y.; Qiu, C. F.; Kwok, H. S.; Zhan, X. W.; Liu, Y. Q.; Zhu, D. B.; Tang, B. Z. Aggregation-induced emission of 1-methyl-1,2,3,4,5-pentaphenylsilole. Chem. Commun. 2001, 18, 1740–1741.
96 Wang, Z.; Yong, T. Y.; Wan, J. S.; Li, Z. H.; Zhao, H.; Zhao, Y. B.; Gan, L.; Yang, X. Y.; Xu, H. B.; Zhang, C. Temperature-sensitive fluorescent organic nanoparticles with aggregation-induced emission for long-term cellular tracing. ACS Appl. Mater. Interfaces 2015, 7(5), 3420–3425.
97 Jiang, B. P.; Tan, X. Y.; Shen, X. C.; Lei, W. Q.; Liang, W. Q.; Ji, S. C.; Liang, H. One-step fabrication of a multifunctional aggregation-induced emission nanoaggregate for targeted cell imaging and enzyme-triggered cancer chemotherapy. ACS Macro Lett. 2016, 5(4), 450–454.
98 Wang, X.; Yang, Y. Y.; Zhuang, Y. P.; Gao, P. Y.; Yang, F.; Shen, H.; Guo, H. X.; Wu, D. C. Fabrication of pH-responsive nanoparticles with an AIE feature for imaging intracellular drug delivery. Biomacromolecules 2016, 17(9), 2920–2929.
99 Shi, H. B.; Kwok, R. T. K.; Liu, J. Z.; Xing, B. G.; Tang, B. Z.; Liu, B. Real-time monitoring of cell apoptosis and drug screening using fluorescent light-up probe with aggregation-induced emission characteristics. J. Am. Chem. Soc. 2012, 134(43), 17972–17981.
100 Jiang, B. P.; Guo, D. S.; Liu, Y. C.; Wang, K. P.; Liu, Y. Photomodulated fluorescence of supramolecular assemblies of sulfonatocalixarenes and tetraphenylethene. ACS Nano 2014, 8(2), 1609–1618.
101 He, Y. G.; Shi, S. Y.; Liu, N.; Ding, Y. S.; Yin, J.; Wu, Z. Q. Tetraphenylethene-functionalized conjugated helical poly(phenyl isocyanide) with tunable light emission, assembly morphology, and specific applications. Macromolecules 2016, 49(1), 48–58.
102 Han, X.; Zhang, J.; Qiao, C. Y.; Zhang, W. M.; Yin, J.; Wu, Z. Q. High-efficiency cell-penetrating helical poly(phenyl isocyanide) chains modified cellular tracer and nanovectors with thiol ratiometric fluorescence imaging performance. Macromolecules 2017, 50(11), 4114–4125.
103 Chen, Y.; Zhang, Z. Z.; Han, X.; Yin, J.; Wu, Z. Q. Oxidation and acid milieu-disintegratable nanovectors with rapid cell-penetrating helical polymer chains for programmed drug release and synergistic chemo-photothermal therapy. Macromolecules 2016, 49(20), 7718–7727.
104 Rajora, A. K.; Ravishankar, D.; Osborn, H. M. I.; Greco, F. Impact of the enhanced permeability and retention (EPR) Effect and cathepsins levels on the activity of polymer-drug conjugates. Polymers 2014, 6(8), 2186–2220.
105 Huang, M. M.; Zhao, K. J.; Wang, L.; Lin, S. Q.; Li, J. J.; Chen, J. B.; Zhao, C. G.; Ge, Z. S. Dual stimuli-responsive polymer prodrugs quantitatively loaded by nanoparticles for enhanced cellular internalization and triggered drug release. ACS Appl. Mater. Interfaces 2016, 8(18), 11226–11236.
106 Hu, X. L.; Hu, J. M.; Tian, J.; Ge, Z. S; Zhang, G. Y.; Luo, K. F.; Liu, S. Y. Polyprodrug amphiphiles: hierarchical assemblies for shape-regulated cellular internalization, trafficking, and drug delivery. J. Am. Chem. Soc. 2013, 135(46), 17617–17629.
107 Hu, X. L.; Liu, G. H.; Li, Y.; Wang, X. R.; Liu, S. Y. Cell-penetrating hyperbranched polyprodrug amphiphiles for synergistic reductive milieu-triggered drug release and enhanced magnetic resonance signals. J. Am. Chem. Soc. 2015, 137(1), 362–368.
108 Cai, K. M.; He, X.; Song, Z. Y.; Yin, Q.; Zhang, Y. F.; Uckun, F. M.; Jiang, C.; Cheng, J. J. Dimeric drug polymeric nanoparticles with exceptionally high drug loading and quantitative loading efficiency. J. Am. Chem. Soc. 2015, 137(10), 3458–3461.
109 Morris, M. C.; Depollier, J.; Mery, J.; Heitz, F.; Divita, G. A peptide carrier for the delivery of biologically active proteins into mammalian cells. Nature Biotechnol. 2001, 19, 1173–1176.
110 Daniels, D. S.; Schepartz, A. Intrinsically cell-permeable miniature proteins based on a minimal cationic PPII motif. J. Am. Chem. Soc. 2007, 129(47), 14578–14579.
111 Smith, B. A.; Daniels, D. S.; Coplin, A. E.; Jordan, G. E.; McGregor, L. M. A. Minimally cationic cell-permeable miniature proteins *via* α-helical arginine display. J. Am. Chem. Soc. 2008, 130(10), 2948–2949.
112 Tang, H. Y.; Yin, L. C.; Kim, K. H.; Cheng, J. J. Helical poly(arginine) mimics with superior cell-penetrating and molecular transporting properties. Chem. Sci. 2013, 4, 3839–3844.
113 Yang, W. H.; Yu, C. M.; Yao, S. Q.; Wu, S. Z. Cell-penetrating poly(disulfide)-based star polymers for simultaneous

intracellular delivery of miRNAs and small molecule drugs. Polym. Chem. 2017, 8, 4043–4051.
114 Green, M. M.; Park, J. W.; Sato, T.; Teramoto, A.; Lifson, S.; Selinger, R. L. B.; Selinger, J. V. The macromolecular route to chiral amplification. Angew. Chem. Int. Ed. 1999, 38(21), 3138–3154.
115 Maeda, K.; Wakasone, S.; Shimomura, K.; Ikai, T.; Kanoh, S. Helical polymer brushes with a preferred-handed helix-sense triggered by a terminal optically active group in the pendant. Chem. Commun. 2012, 48, 3342–3344.
116 Nieh, M. P.; Goodwin, A. A.; Stewart, J. R.; Novak, B. M.; Hoagland, D. A. Chain stiffness of a high molecular weight polyguanidine prepared by living polymerization. Macromolecules 1998, 31(9), 3151–3154.
117 Reuther, J. F.; Bhatt, M. P.; Tian, G.; Batchelor, B. L.; Campos, R.; Novak, B. M.; Controlled living polymerization of carbodiimides using versatile, air-stable nickel(II) initiators: facile incorporation of helical, rod-like materials. Macromolecules 2014, 47(14), 4587–4595.
118 Shi, S. Y.; He, Y. G.; Chen, W. W.; Liu, N.; Zhu, Y. Y.; Ding, Y. S.; Yin, J.; Wu, Z. Q. Polypeptide-*b*-poly(phenyl isocyanide) hybrid rod-rod copolymers: one-pot synthesis, self-assembly, and cell imaging. Macromol. Rapid Commun. 2015, 36(16), 1511–1520.
119 He, Y. G.; Shi, S. Y.; Liu, N.; Zhu, Y. Y.; Ding, Y. S.; Yin, J.; Wu, Z. Q. Fabrication of SERS-active conjugated copolymers/gold nanoparticles composite films by interface-directed assembly. RSC Adv. 2015, 5, 39697–39704.
120 Li, W.; He, Y. G.; Shi, S. Y.; Liu, N.; Zhu, Y. Y.; Ding, Y. S.; Yin, J.; Wu, Z. Q. Fabrication of a multi-charge generable poly(phenyl isocyanide)-block-poly(3-hexylthiophene) rod-rod conjugated copolymer. Polym. Chem. 2015, 6, 2348–2355.
121 Yin, J.; Xu, L.; Han, X.; Zhou, L.; Li, C. L.; Wu, Z. Q. A facile synthetic route to stereoregular helical poly(phenyl isocyanide)s with defined pendants and controlled helicity. Polym. Chem. 2017, 8, 545–556.
122 Zhang, Z. Z.; Qiao, C. Y.; Zhang, J.; Zhang, W. M.; Yin, J.; Wu, Z. Q. Synthesis of unimolecular micelles with incorporated hyperbranched boltorn h30 polyester modified with hyperbranched helical poly(phenyl isocyanide) chains and their enantioselective crystallization performance. Macromol. Rapid Commun. 2017, 38, DOI: 10.1002/marc.201700315
123 Engelkamp, H.; Middelbeek, S.; Nolte, R. J. M. Self-assembly of disk-shaped molecules to coiled-coil aggregates with tunable helicity. Science, 1999, 284(5415), 785–788.
124 Kajitani, T.; Onouchi, H.; Sakurai, S. I.; Nagai, K.; Okoshi, K.; Onitsuka, K.; Yashima, E. Latticelike smectic liquid crystal phase in a rigid-rod helical polyisocyanide with mesogenic pendants. J. Am. Chem. Soc. 2011, 133(24), 9156–9159.
125 Xu, A. Q.; Hu, G. X.; Hu, Y. L.; Zhang, X. Q.; Liu, K.; Kuang, G. C.; Zhang, A. F. Remarkable structure effects on chiroptical properties of polyisocyanides carrying proline pendants. Chem. Asian J. 2013, 8(9), 2003–2014.

https://doi.org/10.1007/s10118-018-2035-9